https://doi.org/10.5194/egusphere-2026-3097
Preprint. Discussion started: 23 June 2026

A Lagrangian framework to simulate *Sargassum* transport and growth

Elena Gianotten[1], Meike F. Bos[1], Darshika Manral[1,2], Fabio Nauer[3], Erik Zettler[3], Linda A. Amaral-Zettler[3,4], and Erik van Sebille[1]

[1]Institute for Marine and Atmospheric research, Utrecht University, Utrecht, Netherlands
[2]Deltares, Department of Data Science and Water Quality, Delft 2600 MH, The Netherlands
[3]Royal Netherlands Institute for Sea Research, Den Burg, Netherlands
[4]Institute for Biodiversity and Ecosystem Dynamics, University of Amsterdam, Amsterdam, The Netherlands

Correspondence: Erik van Sebille (E.vanSebille@uu.nl)

Abstract. Blooms of the seaweed *Sargassum* have been reported in the Tropical Atlantic Ocean and Caribbean Sea since 2011. Large-scale inundation events of this seaweed in coastal regions have a negative impact on both the economy and the environment. To predict the timing, location and quantity of *Sargassum* strandings, model frameworks that link open ocean distributions to coastal regions are required. Here, we develop an open-source customizable Lagrangian simulation framework and growth model for *Sargassum* that combines transport by currents, wind and waves with a biological modelling framework that includes dynamic growth limitation depending on temperature, nitrate availability and salinity. The framework can use satellite detections of the *Sargassum* Watch System (SaWS) to initialise virtual *Sargassum* particles in the Tropical Atlantic Ocean. We demonstrate that the combination of physical transport and biological growth strongly affects *Sargassum* distribution, with substantial variability on spatio-temporal scales. We show that temperature is the strongest growth-limiting parameter, and in particular that elevated surface temperatures, together with low salinity from the Amazon River plume, play a crucial role in *Sargassum* decline.

1 Introduction

The Sargasso Sea is a region in the North Atlantic Ocean that has been named after a brown, floating seaweed species, called *Sargassum* (Phaeophyceae, Ochrophyta). While *Sargassum* had been abundant in the Sargasso Sea for centuries, a recent shift has occurred. Since 2011, large blooms of *Sargassum* have been reported in the Atlantic Ocean and the Caribbean Sea (Wang et al., 2019). Pelagic *Sargassum* in the tropical Atlantic comprises two species – *S. fluitans* (Børgesen) Børgesen and *S. natans* (Linnaeus) Gaillon – which together include three dominant genotypes: *S. fluitans* III, *S. natans* I, and *S. natans* VIII. Although early classifications were based on morphology (Winge, 1923; Parr, 1939), recent genetic studies confirm that these forms represent closely related but distinct lineages (Amaral-Zettler et al., 2017).

In recent years, the widespread presence of *Sargassum* in the tropical Atlantic has led to large-scale beaching events and was also detected by satellites using remote sensing techniques (Gower et al., 2013; Amaral-Zettler et al., 2017; Debue et al., 2025). As the *Sargassum* distribution extends from the Gulf of Mexico to West Africa, it is referred to as the Great Atlantic

https://doi.org/10.5194/egusphere-2026-3097
Preprint. Discussion started: 23 June 2026

Sargassum Belt (Wang et al., 2019). Although 15 years of multidisciplinary research has improved our understanding of the timing and causes of these blooms, uncertainty remains regarding their specific drivers and projections (Editors, 2025).

Although *Sargassum* rafts in the open ocean contribute positively to the diversity of pelagic habitats (van Tussenbroek et al., 2024), *Sargassum* beaching events can create low-light and hypoxic or anoxic conditions, thereby negatively impacting coastal regions (Van Tussenbroek et al., 2017). Such events have occurred on the coastlines of Caribbean Islands, the Gulf of Mexico, northern Brazil and the western coast of Africa and impact tourism, the fishing industry, human health and local coastal environments (Chávez et al., 2020; Oxenford et al., 2021; Debue et al., 2025).

To limit the negative impacts of *Sargassum* inundation events, accurate predictions of timing, location and quantity of strandings are required. Two complementary methods have been developed for this: firstly, remote sensing, to detect *Sargassum* accumulations in the open ocean and secondly, modelling, to forecast *Sargassum* transport and growth (Debue et al., 2025). Here, we develop a framework that combines the two, and focuses on the modelling component. Understanding *Sargassum* dynamics and eventually predicting strandings requires combining the physical transport and biological growth and mortality of *Sargassum* rafts (Marsh et al., 2021; Jouanno et al., 2021; Corbin and Oxenford, 2023; Bonner et al., 2024; Debue et al., 2025; Beron-Vera et al., 2026).

Near-surface ocean circulation is the primary mechanism driving the spatial distribution of *Sargassum* in the Atlantic Ocean (Wang et al., 2019). As *Sargassum* rafts float on the surface, the direct effects of wind (windage) and waves (Stokes drift) also influence their movement (Putman et al., 2020; Manral, 2025). Interactions between the morphological properties of *Sargassum* rafts and physical transport mechanisms cause biophysical feedbacks. These feedbacks complicate modelling of raft dynamics, as the variation in size, mass and density of *Sargassum* rafts in turn affect the transport mechanisms (Brooks et al., 2019; Putman et al., 2020; Marsh et al., 2022; Bonner et al., 2024; Beron-Vera et al., 2026).

While *Sargassum* can have high growth rates, unfavourable physico-chemical conditions can strongly limit this rate. This growth limitation has been included in models before, for example in Jouanno et al. (2021), Podlejski et al. (2024), Bonner et al. (2024), and Jouanno et al. (2025). Empirical studies of pelagic *Sargassum* morphotypes have demonstrated remarkably high growth rates, including biomass doublings within a two-week period (Corbin and Oxenford, 2023; Magaña-Gallegos et al., 2023b). One of the main hypotheses of the *Sargassum* bloom in the Tropical Atlantic is thus the favorable environmental conditions there, such as high nutrient input from upwelling waters, Saharan dust deposition, and river outflows, and the elevated temperatures linked to climate change (Wang et al., 2019). However, variability in observed growth rates is high because environmental (physico-chemical) conditions such as temperature, salinity, nutrient availability, and incoming solar radiation influence *Sargassum* growth (Hanisak and Samuel, 1987; Debue et al., 2025; Magaña-Gallegos et al., 2023b). Furthermore, *Sargassum* growth rates vary among different genotypes (Corbin and Oxenford, 2023; Magaña-Gallegos et al., 2023b) and conducting growth experiments on these pelagic organisms under controlled conditions is difficult, because it is challenging to keep the organisms alive in culture (Magaña-Gallegos et al., 2023a).

In the context of these challenges, our primary aim is to develop a customizable *Sargassum* growth model that can be implemented in a Lagrangian ocean modelling framework to compute *Sargassum* growth during transport. We then use this framework to explore the sensitivity of the basin-scale distribution of *Sargassum* to inclusion of a biological growth model

https://doi.org/10.5194/egusphere-2026-3097
Preprint. Discussion started: 23 June 2026

and transport for the year 2024. The variety in reported growth rates, physiological differences between morphotypes and uncertainty regarding growth limitation by physico-chemical factors underline the relevance of such a customizable framework, which could bridge between modelling studies and experimental studies.

2 Methods

2.1 Horizontal transport

We use Parcels v4.0.0 (Delandmeter and Van Sebille, 2019) to simulate the dispersion of virtual *Sargassum* raft particles in the Atlantic Ocean, as they are advected by ocean currents, Stokes drift, and direct wind-induced drag (windage). The horizontal displacement of a virtual *Sargassum* raft particle is calculated by:

$$\boldsymbol{x}(t+\Delta t) = \boldsymbol{x}(t) + \int_{t}^{t+\Delta t} \left(\boldsymbol{v}_{ocean}(\boldsymbol{x},\tau) + \boldsymbol{v}_{Stokes}(\boldsymbol{x},\tau) + \boldsymbol{v}_{wind}(\boldsymbol{x},\tau)\right) d\tau, \tag{1}$$

where $\boldsymbol{x}(t)$ is the position of the particle at a simulated time t. $\boldsymbol{v}_{ocean}(\boldsymbol{x},\tau)$ is the corresponding horizontal surface velocity, based on a hydrodynamic velocity field of the ocean, $\boldsymbol{v}_{Stokes}(\boldsymbol{x},\tau)$ is the horizontal velocity due to wave-driven Stokes drift, and $\boldsymbol{v}_{wind}(\boldsymbol{x},\tau)$ is the horizontal velocity due to direct windage. The integral is solved using 2nd order Runge-Kutta integration, with a timestep of 10 minutes.

For the coastal boundary conditions, particles are considered stranded when they reach a grid cell where the zonal or meridional ocean velocity is exactly 0. The transport and growth of these stranded particles are stopped. Table B1 gives an overview of all the default simulation settings, which will be further explained in the rest of this section.

2.1.1 Stokes drift

As *Sargassum* rafts float on the surface, they are exposed to waves and therefore to wave-induced Stokes drift (Stokes, 1847; van den Bremer and Breivik, 2018), where a parcel on the surface will experience a net drift velocity in the direction of wave propagation. However, unlike for example microplastics or phytoplankton, *Sargassum* rafts cannot be treated as passive, point-like particles (Beron-Vera, 2021). This large vertical extent of *Sargassum* rafts and its variability over space and time complicates incorporating a realistic Stokes drift component.

The vertical extent of *Sargassum* rafts is typically between 0.1 and 0.5 m with a maximum of 1 m (Ody et al., 2019). Manral (2025) measured depth extents of *Sargassum* rafts ranging from 0.1 to 0.8 m during the *Weeds of Change* research expedition 64PE535 aboard the *R/V Pelagia*, in the northern tropical Atlantic between Pointe-à-Pitre, French Antilles and Mindelo, Cabo Verde, from June 13 to July 12, 2024.

Here, we compute the depth-dependent Stokes drift by integrating the vertical Stokes drift profile over the vertical extent of the raft. The analytical solution for the vertically integrated Stokes decay function based on a Philips spectrum was derived by

https://doi.org/10.5194/egusphere-2026-3097
Preprint. Discussion started: 23 June 2026

Li et al. (2017). The resulting depth-integrated Stokes drift velocity of a *Sargassum* raft, $\boldsymbol{v}_{Stokes}(\boldsymbol{x},\tau)$ is given by:

$$\boldsymbol{v}_{Stokes}(\boldsymbol{x},t) = \boldsymbol{v}_{Stokes}\left(\boldsymbol{x}_{z=0},t\right)\frac{D\left(z_{lower},k_p\right) - D\left(z_{upper},k_p\right)}{z_{lower} - z_{upper}}, \tag{2}$$

where $\boldsymbol{v}_{Stokes}(\boldsymbol{x}_{z=0},t)$ is the wave-induced Stokes drift velocity at the ocean surface. Depth extent z is defined positive downward, with z = 0 at the ocean surface. The function $D(z,k_p)$ is the vertically integrated Stokes decay factor and is given by:

$$D(z,k_p) = \frac{1}{2k_p}\left[1 - e^{-2k_p z} - \frac{2\beta}{3}\left[1 + \sqrt{\pi}\left(2k_p z\right)^{3/2}\operatorname{erfc}\left(\sqrt{2k_p z}\right) - \left(1 + 2k_p z\right)e^{-2k_p z}\right]\right], \tag{3}$$

where $k_p = \omega_p^2/g$ and $\omega_p = 2\pi/T_p$, with $g = 9.81\ \mathrm{m\ s^{-2}}$. Here, k_p is the peak wave number, ω_p is the peak wave frequency and T_p is the peak wave period. The parameter β = 1, corresponding to a Phillips spectrum and erfc denotes the complementary error function.

For the rest of this study, we use $z_{upper} = 0\ \mathrm{m}$ and $z_{lower} = 1\ \mathrm{m}$ as the upper and lower extents of the *Sargassum* raft, although these parameters are user-adjustable in the framework. The analytical results of the depth-integrated Stokes drift are shown in Figure A1, which illustrates the decay of Stokes drift with increasing vertical extent of a raft for different wave periods.

2.1.2 Windage

Due to the buoyant nature of *Sargassum*, rafts are slightly exposed above the water column, causing *Sargassum* rafts to experience an additional force from wind-induced drag; also called leeway (Allen and Plourde, 1999; Johns et al., 2020; Marsh et al., 2021; Podlejski et al., 2024; Johnson et al., 2020; Putman et al., 2020; Van Sebille et al., 2021):

$$\boldsymbol{v}_{wind} = c\left(\boldsymbol{v}_{wind_{10}} - \boldsymbol{v}_{ocean}\right), \tag{4}$$

where $\boldsymbol{v}_{wind_{10}}$ is the wind speed 10 m above the surface. Estimates of the windage parameter c typically range from $c = 0.33\%$ to $c = 3\%$ for *Sargassum* (Debue et al., 2025). In this study, we use a windage coefficient of $c = 1\%$ of the relative wind speed (see also Table B1).

2.2 Biological growth

In experimental studies, *Sargassum* growth rates are commonly calculated according to the formulation of Hanisak and Samuel (1987):

$$\mu = \frac{\log_2(W_t/W_i)}{t}, \tag{5}$$

where, μ is the specific growth rate expressed as doublings per day, based on the initial weight of the plant (W_i) and the weight at time t (W_t). By basing our biological modelling framework on this empirical expression, we facilitate direct implementation of measured specific growth rates. Our base variable is biomass change (in percentage) rather than absolute biomass:

$$B(t+\Delta t) = B(t)\ 2^{(f\mu_{\max} - m)\Delta t}, \tag{6}$$

https://doi.org/10.5194/egusphere-2026-3097
Preprint. Discussion started: 23 June 2026

where B is the biomass change of a particle, $\mu_{\max}$ is the maximum specific growth rate of *Sargassum*, f is the local total growth factor, m is a mortality rate and Δt the time step of the simulation.

Here, we use $\mu_{\max} = 0.095\ \mathrm{day}^{-1}$, which is the maximum specific growth rate for *S. fluitans III*, measured by Magaña-Gallegos et al. (2023b). To avoid negative values of biomass, the mortality term $m = 0.025\ \mathrm{day}^{-1}$ is proportional to B.

The total growth factor f varies in time and space, within a range of $[0, 1]$. It is a multiplication of three growth factor functions that prescribe *Sargassum* growth under influence of temperature (T), external nitrogen availability (N) and salinity (S):

$$f = f_T \cdot f_N \cdot f_S. \tag{7}$$

All growth factor functions can have a maximum value of 1, indicating no growth limitation and optimal growth conditions; and a minimum value of 0, indicating total growth limitation and no growth.

2.2.1 Temperate limitation

The dependency of *Sargassum* growth on temperature is based on laboratory culture experiments of *Sargassum* under varying sea surface temperatures (Hanisak and Samuel, 1987; Magaña-Gallegos et al., 2023b). Following, Jouanno et al. (2025) it is given by:

$$f_T = \begin{cases} \exp\left(-2\left(\dfrac{T(\boldsymbol{x},t) - T_{\mathrm{opt}}}{T_{\min} - T_{\mathrm{opt}}}\right)^2\right), & T(\boldsymbol{x},t) \le T_{\mathrm{opt}}, \\ \exp\left(-2\left(\dfrac{T(\boldsymbol{x},t) - T_{\mathrm{opt}}}{T_{\max} - T_{\mathrm{opt}}}\right)^2\right), & T(\boldsymbol{x},t) > T_{\mathrm{opt}}, \end{cases} \tag{8}$$

where $T(\boldsymbol{x},t)$ is the local temperature experienced by the particle, T_{opt} is the optimal temperature for *Sargassum* growth, and $T_{\min}$ and $T_{\max}$ are the minimum and maximum temperatures allowing *Sargassum* growth. The values used in this study are listed in Table B1), but they are user-adaptable in the framework to facilitate exploration of the sensitivity to growth and selected subspecies.

2.2.2 Nitrogen limitation

The response of *Sargassum* to the external availability of the nutrient nitrogen is also incorporated into the biological modelling framework. In the ocean, dissolved nitrogen is predominantly present in the form of nitrate (NO_3^-). Following the approach of Bonner et al. (2024), a dependence of *Sargassum* on external nitrate availability is included via the Monod equation. This is an empirical mathematical model for the growth of organisms and is modelled as:

$$f_N = \frac{[NO_3^-](\boldsymbol{x},t)}{k_N + [NO_3^-](\boldsymbol{x},t)} \tag{9}$$

where $[NO_3^-](\boldsymbol{x},t)$ is the local nitrate concentration experienced by the particle and k_N is the nitrate uptake half saturation, also referred to as the half velocity constant. This parameter defines the nitrate concentration at which the growth rate is reduced to half of its maximum value ($\mu/\mu_{max} = 0.5$).

https://doi.org/10.5194/egusphere-2026-3097
Preprint. Discussion started: 23 June 2026

Bonner et al. (2024) used a value of $k_N = 0.000129\,\mathrm{mmol\,m^{-3}}$, to optimize for their specific model configuration. However, this value was not empirically derived and is relatively low compared to typical nitrate concentrations. Given the sensitivity of growth to the choice of k_N, its value remains uncertain. Therefore, we conducted a sensitivity analysis to assess the influence of k_N on model behaviour and to derive a suitable parameter value (see Section 3.1.2).

2.2.3 Salinity limitation

Finally, Hanisak and Samuel (1987) reported a strong reduction of growth of pelagic *Sargassum* species under low salinity conditions. To capture this observed behaviour, we use the formulation of Jouanno et al. (2025):

$$f_S = \exp\left(-0.02\left(S_{\mathrm{opt}} - S(\boldsymbol{x},t)\right)^2\right), \tag{10}$$

where $S(\boldsymbol{x},t)$ is the local salinity experienced by the particle and S_{opt} is the optimal salinity.

The *Sargassum* growth factor dependencies described by Equations (8), (9) and (10) for *S. fluitans* are visualised in Figure A2. The associated default model parameters used here can be found in Table B1. We focus here on *S. fluitans* due to the availability of data in the literature and the significantly higher abundance of *S. fluitans* over *S. natans* in the rafts (70% vs. 30%, respectively) during the expedition.

2.3 Hydrodynamic and biogeochemical datasets

The hydrodynamic and biogeochemical data used in our framework comes from the Copernicus Marine Service (E.U. Copernicus Marine Service Information, 2024a, b, c). The wind velocities come from the Copernicus Climate Data Store (Hersbach et al., 2023). See Table B2 for an overview of the variables and models that were utilized, together with the associated sources, spatial resolutions, temporal resolutions and types of grid. Most of the datasets have a 1/12° horizontal resolution, which is much larger than the typical size of *Sargassum* rafts (Ody et al., 2019).

As we focus on the surface transport of *Sargassum*, we only use the uppermost grid layer of the ocean models, which has an extent of $1.011\mathrm{m}$ – thicker than the raft depth extents mentioned by Ody et al. (2019) and Manral (2025).

2.4 Particle initialisation

2.4.1 Satellite-based initialisation

To initialise *Sargassum* particles at locations where actual *Sargassum* has been detected, our framework can use satellite images of the *Sargassum* Watch System (SaWS) of the University of South-Florida. The SaWs composite FA-UNET-DENSITY-7DAY images provide floating algae density at a spatial resolution of $\sim 1\ \mathrm{km}$ (see the top row in Figure 1 for three example images). The density of floating algae is calculated as a mean of the past seven days, and is based on the U-Net method described by Hu et al. (2023). Black pixels in the images indicate insufficient data due to clouds.

We convert a composite of all twelve of these SaWs images to a release map of virtual *Sargassum* raft particles through the following steps: First, the RGB value and brightness are computed for every pixel. A brightness threshold of 60 was

https://doi.org/10.5194/egusphere-2026-3097
Preprint. Discussion started: 23 June 2026

determined manually to include all pixels showing *Sargassum* while effectively excluding ocean water and cloud-covered areas. Additionally, a dilated landmask based on the brown colour of the image was created to filter pixels on land and within 20 km (corresponding to approximately 2 grid cells of input data) from the coast. This ensures that particles are only initialised in the open ocean. Finally, a virtual particle is initiated at every 8th pixel (so at every 8 km) where *Sargassum* is detected (Figure 1) – which is the resolution of the hydrodynamic model data.

Here, the virtual *Sargassum* particles are released uniformly and with equal $B(0)$. While information on *Sargassum* abundance is lost this way, it avoids having to introduce an unknown scaling between density of floating algae and *Sargassum* biomass. This is a common approach in Lagrangian modelling of *Sargassum* (Debue et al., 2025). The interactive notebook supports changing the $B(0)$ on a per-particle level.

2.4.2 Basin-wide initialisation

For spatio-temporal analyses on a basin scale, we also create a larger release grid, spanning the region (100°W, 25°S) to (16°E, 45°N). We release 17,871 virtual particles uniformly at every 1/2° within the Atlantic Ocean on the first day of each month in 2024.

3 Results

3.1 Satellite-based simulations

3.1.1 Validation of Lagrangian transport

Our primary focus in this study is on *Sargassum* transport and growth in July 2024, to allow comparison with experimental results of *R/V Pelagia* Expedition 64PE535 (part of Weeds of Change project). To validate the transport model, we perform a model simulation initialised from the SaWS satellite images on 1 July 2024 and compare the distribution of simulated particles after 31 days with the *Sargassum* distribution detected by the SaWS one month later on 1 August 2024 (Figure 2).

While the virtual particle distribution is slightly more converged than the satellite distribution, the distributions in Figure 2 agree reasonably well. The simulation captures the areas of *Sargassum* convergence in the Central Atlantic (55°W-15°W in Figure 2) especially well. The simulation shows higher *Sargassum* spread north of 20°N, but this could also be a bias in the satellite detection due to to cloud coverage in that region at the release date (black in Figure 1b). A total of 171 particles (2.11% of the 8096 released) have stranded, mostly on the Northern Caribbean Islands and the West African coast.

3.1.2 Optimizing nitrate dependency of growth model

To define a suitable nitrate dependency for the growth model, we examine the nitrate conditions encountered by the particles during transport by computing the temporal mean nitrate concentration sampled along each trajectory. The resulting distribution of mean nitrate concentrations is shown in Figure 3a.

https://doi.org/10.5194/egusphere-2026-3097
Preprint. Discussion started: 23 June 2026

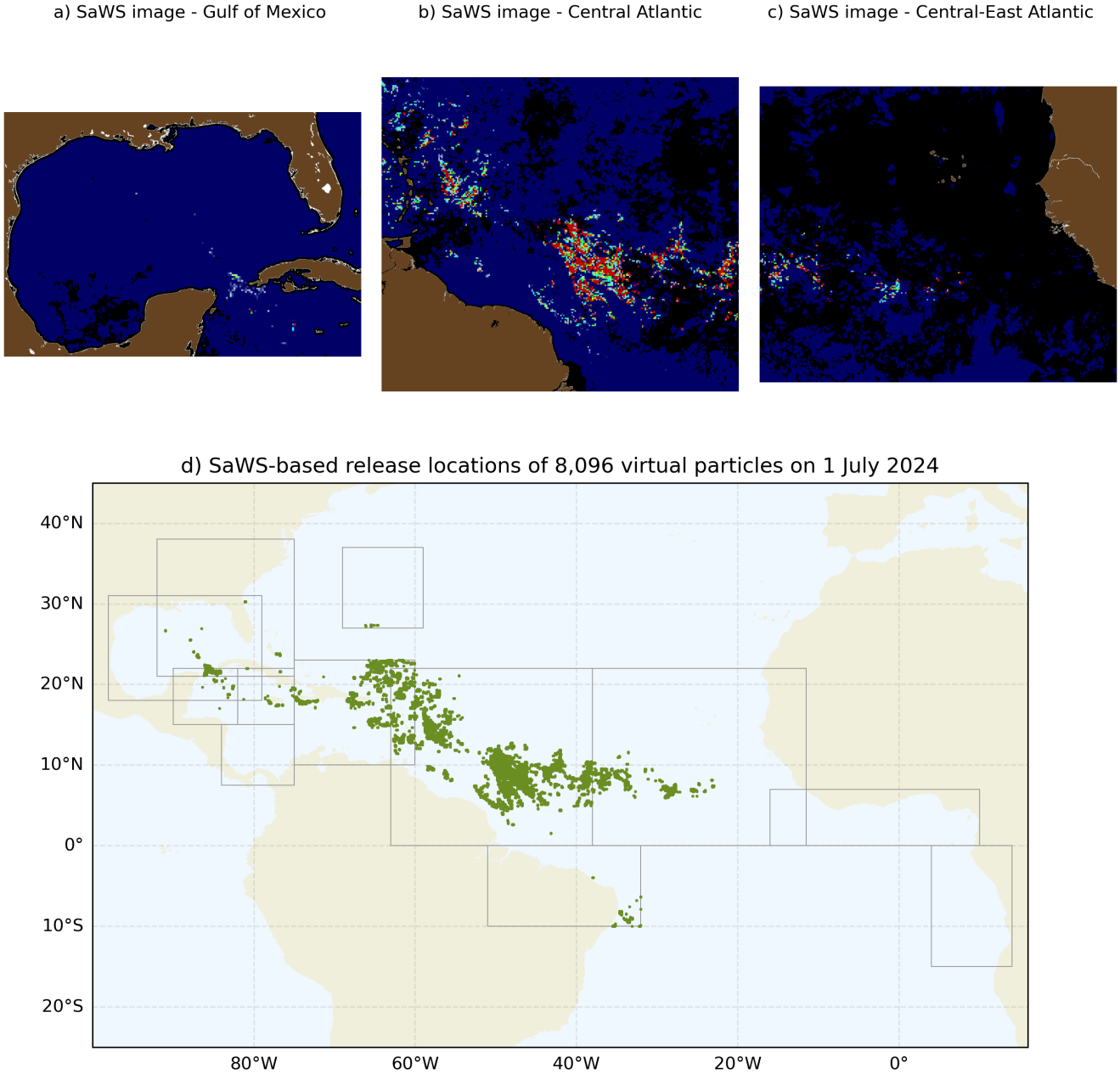

Figure 1. Three of the twelve SaWS satellite images (a-c) used to create a map(d) of release locations for virtual *Sargassum* particles (green dots). Black pixels in satellite images (a-c) indicate that there is insufficient data due to clouds. The grey rectangles on the map (d) indicate the twelve regions for which SaWS satellite images are available.

https://doi.org/10.5194/egusphere-2026-3097
Preprint. Discussion started: 23 June 2026

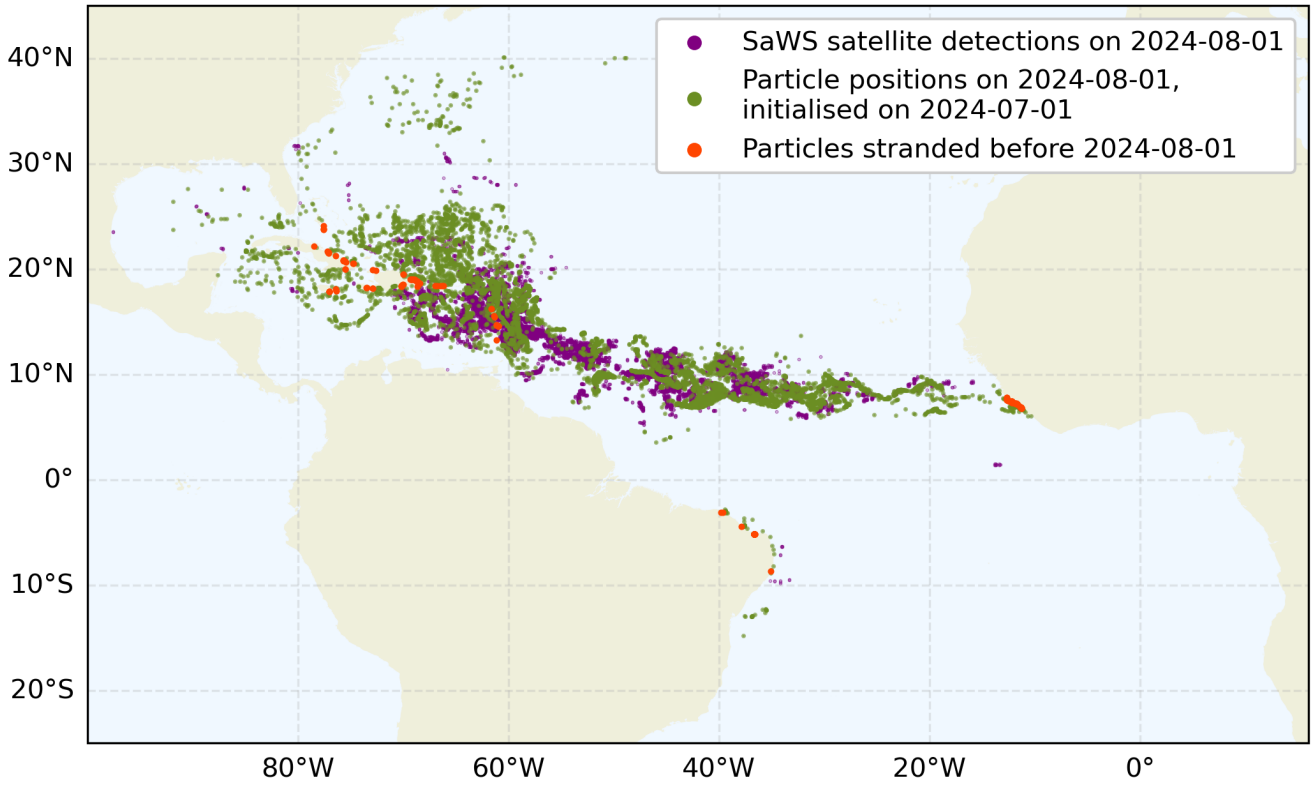

Figure 2. Converted *Sargassum* distribution detected by SaWS on 1 August 2024 (purple) and simulated *Sargassum* particle distribution on 1 August 2024 initialised on 1 July 2024 (green). Particles in red have stranded before the end of the simulation. These account for 2.11% of all particles.

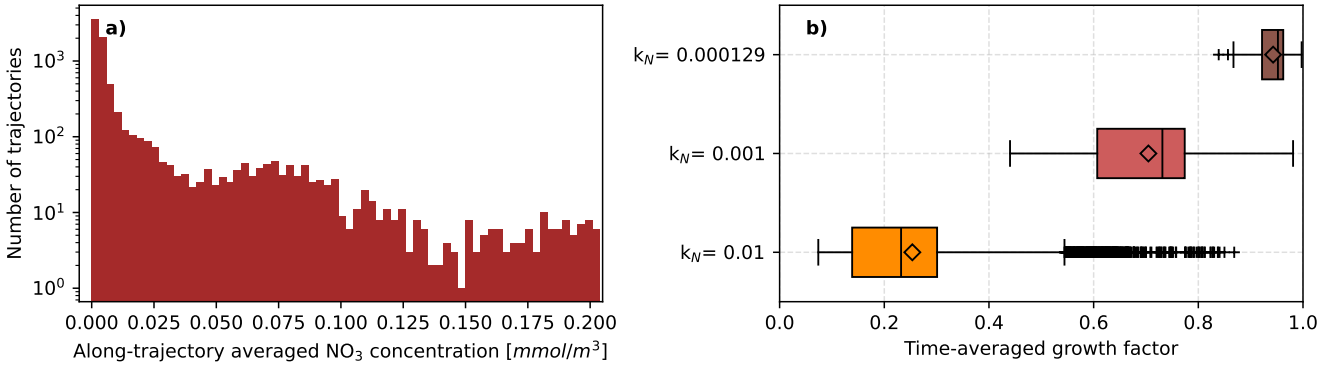

Figure 3. Analysis of the nitrate growth model. a) Distribution of time-averaged nitrate concentrations sampled along trajectories, shown with a logarithmic y-axis. b) Boxplots of time-averaged nitrate growth factor over trajectory for simulations with different uptake half saturation values (k_N in $\mathrm{mmol\ m^{-3}}$). Vertical lines indicate medians and diamonds indicate means.

https://doi.org/10.5194/egusphere-2026-3097
Preprint. Discussion started: 23 June 2026

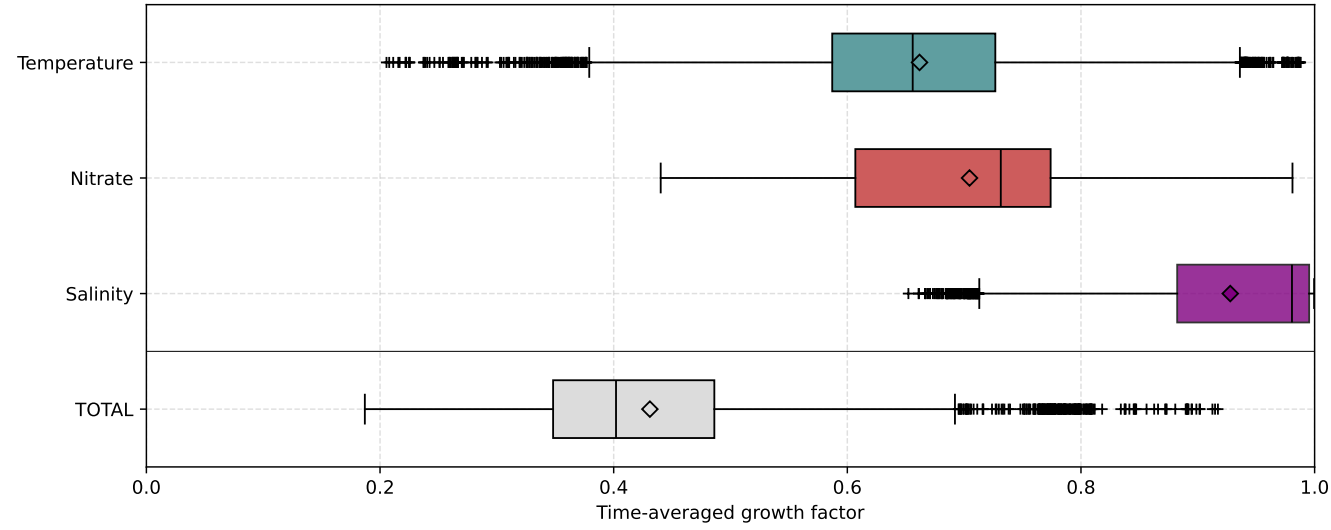

Figure 4. Boxplots of time-averaged total growth factor and time-averaged growth factors of temperature, nitrate and salinity for the simulation with $k_N = 0.001$ mmol m^{-3}. Vertical lines indicate medians and diamonds indicate means.

To assess how *Sargassum* growth responds to the choice of k_N, we perform three simulations with different values of k_N: with $k_N = 0.000129$ mmol m^{-3} (Bonner et al., 2024), with $k_N = 0.001$ mmol m^{-3}, and with $k_N = 0.01$ mmol m^{-3}. Note that we use mmol m^{-3} throughout this study, as this is the units in which the nitrate fields are provided in the Copernicus Marine Service datasets. We compute the time-averaged nitrate growth factor along the trajectory of each virtual particle, initialised based on the SaWs map of 1 July 2024.

The distributions of time-averaged nitrate growth factors (Figure 3b) shows that $k_N = 0.000129$ mmol m^{-3}, as applied in Bonner et al. (2024), results in a very high time-averaged growth factor; implying that *Sargassum* growth is hardly limited by nitrate. In contrast, a k_N-value of 0.01 mmol m^{-3} results in a very strong growth limitation, making nitrate availability unrealistically restrictive. The simulation with $k_N = 0.001$ mmol m^{-3}, gives an intermediate response with growth limitations of 0.6–0.8; and we choose this value for the rest of our simulations. Note, however, that the value of k_N can readily be adapted in our open-source notebook at https://doi.org/10.5281/zenodo.20441020.

3.1.3 Growth limitation and biomass change

To further evaluate this choice of k_N, we compare the along-trajectory growth factors of temperature, nitrate and salinity (Figure 4). The boxplots show that, for these parameter choices, the growth-limiting effect of nitrate availability is slightly weaker than the growth-limiting effect of temperature, but stronger than that of salinity. The total growth factor (bottom boxplot in Figure 4) indicates that the total growth is substantially limited, with typical growth at only 40% of the maximum possible growth. Other studies have also found that temperature is the most important limitation to growth, followed by nitrate and then salinity (Wang et al., 2019; Magaña-Gallegos et al., 2023a; Podlejski et al., 2024; Debue et al., 2025).

https://doi.org/10.5194/egusphere-2026-3097
Preprint. Discussion started: 23 June 2026

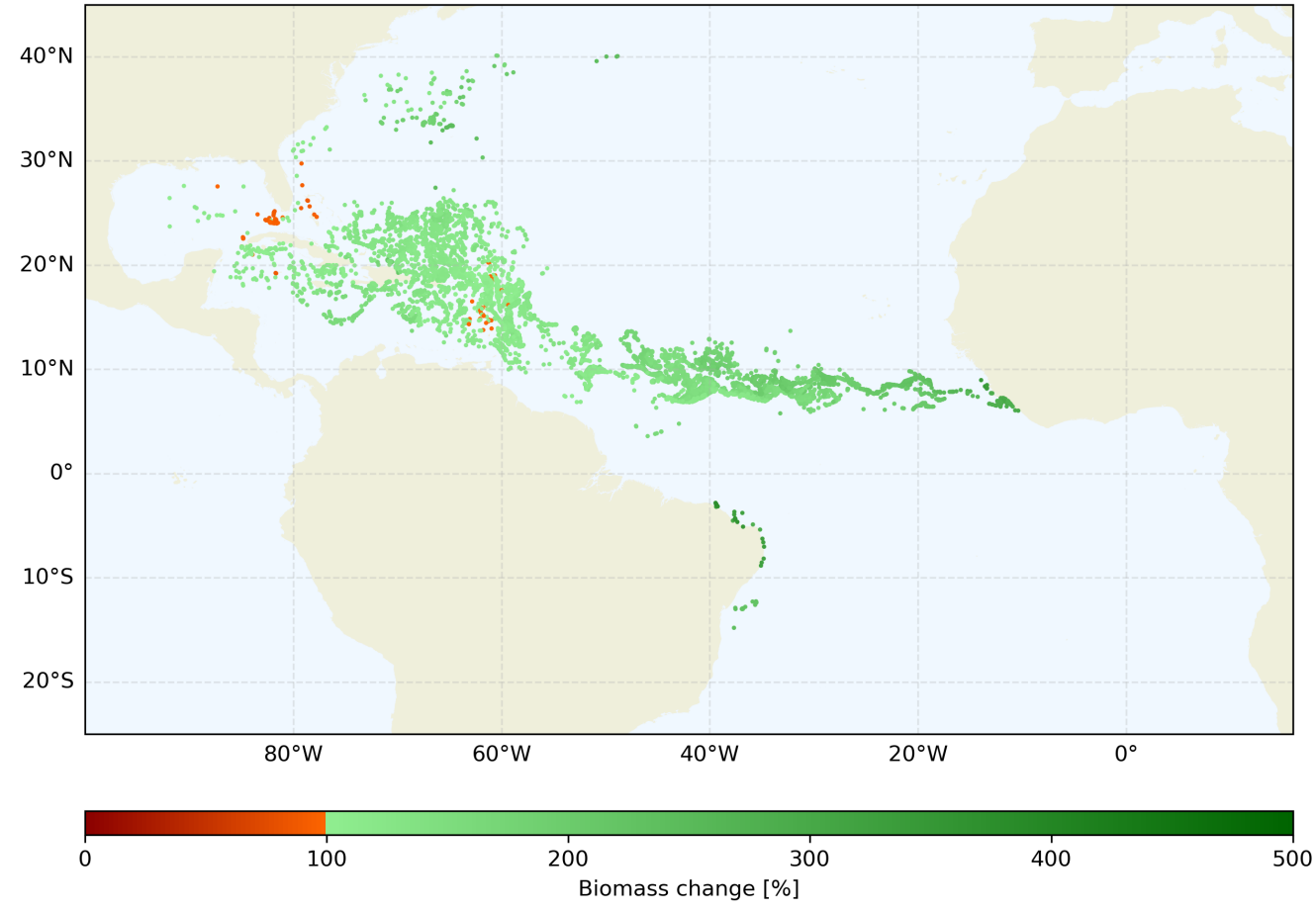

Figure 5. Change in biomass of virtual *Sargassum* particles on 1 August 2024, relative to their initial biomass on 1 July 2024. Each particle is plotted at their final location on 1 August 2024.

The biomass change (B) of virtual *Sargassum* particles during transport (Figure 5) shows spatial variation throughout the Atlantic Ocean. The biomass of all the virtual particles has increased by the end of the simulation, with an average of 145%. Only 1.4% of the virtual particles experience a decrease in biomass (red particles in Figure 5), mostly around Florida and the Northeast Caribbean Islands, while the biomass change is more than 300% near Africa. In general, biomass increases going eastward.

3.2 Basin-wide simulations

To put the results of the simulation of satellite-based particle initialisation for July 2024 into a broader spatial and temporal perspective, we also compute the biomass change for the entire (sub)tropical Atlantic Ocean and for each month in 2024 (Fig-

https://doi.org/10.5194/egusphere-2026-3097
Preprint. Discussion started: 23 June 2026

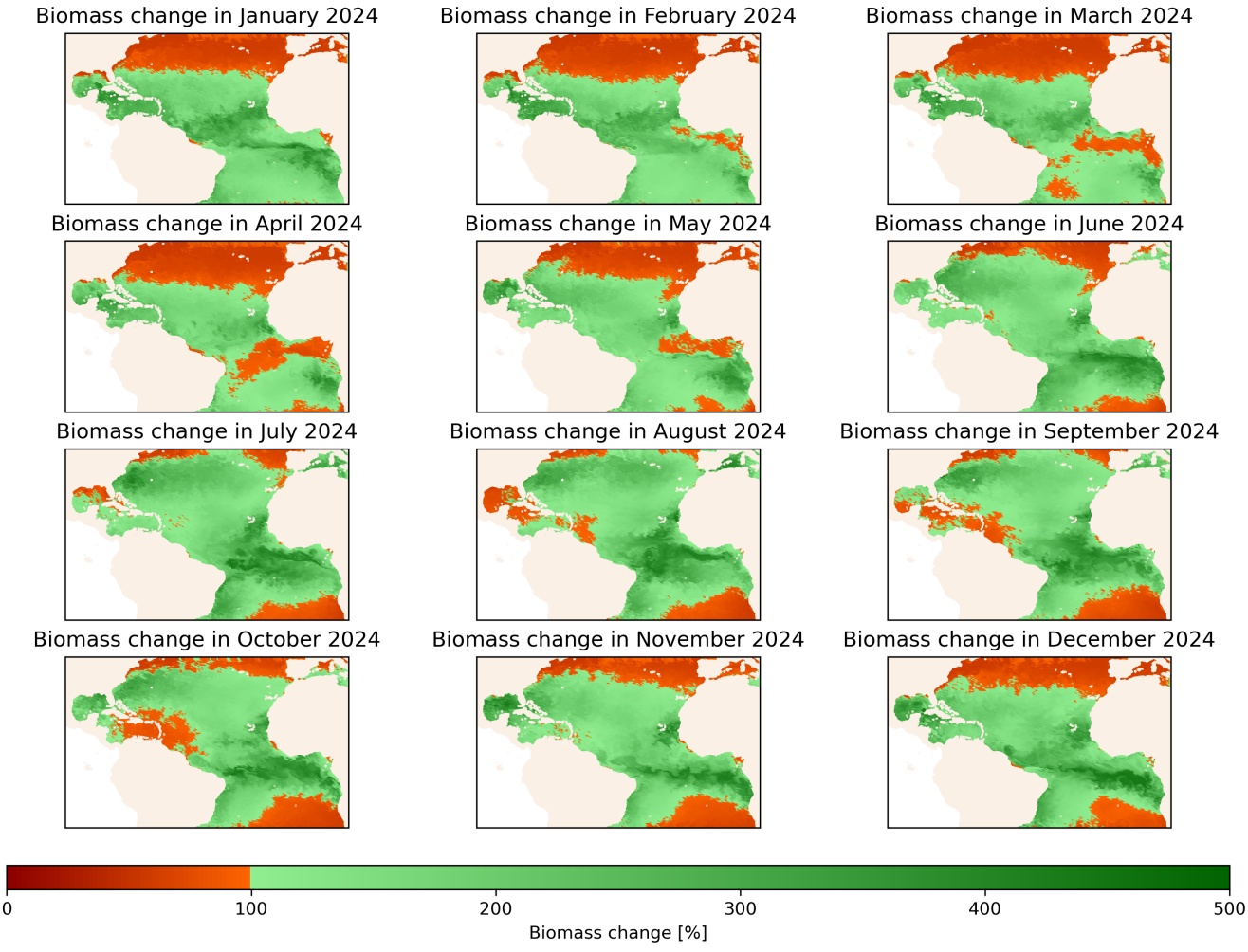

Figure 6. Maps of biomass change after 31 days of simulations for the entire (sub)tropical Atlantic Ocean. Particles are plotted at their initial location. Green values above 100% indicate an increase of biomass over the 31 days; red values below 100% indicate a decrease in biomass. The twelve simulations are started on the first day of every month in 2024.

ure 6). In general, these maps of biomass change reveal strong spatial and temporal variability in growth conditions throughout the (sub)tropical Atlantic.

230 Virtual *Sargassum* particles that start in the dark green areas experience changes in biomass of up to 400–500% within one month. Such regions are present throughout the year near the Cape Verde Islands and along the Equatorial Atlantic between June and January. Particles that start in the Caribbean Sea and the central Atlantic Ocean between November and June also experience biomass increases, with values higher than 200% between November and April.

https://doi.org/10.5194/egusphere-2026-3097
Preprint. Discussion started: 23 June 2026

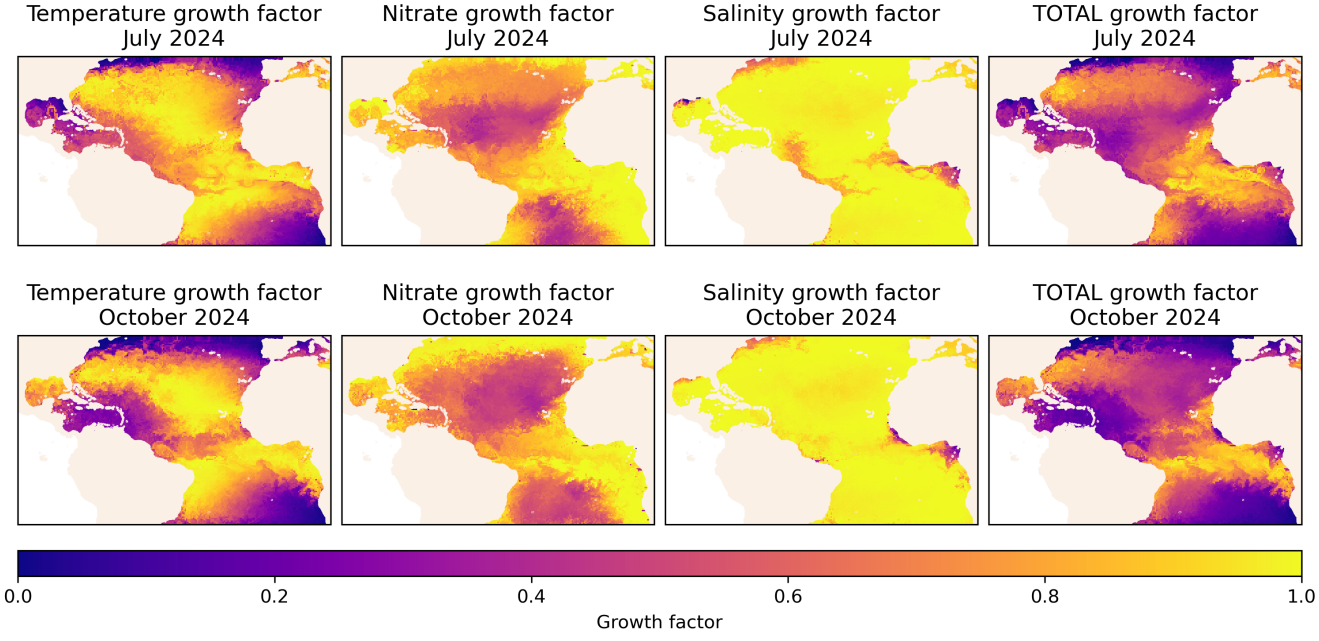

Figure 7. Spatial maps of the along-trajectory growth factors of temperature (f_T; left column), nitrate (f_N; second column) and salinity (f_S; third column), as well as the total growth factor (f; wight column) for particles released on 1 July 2024 and 1 October 2024. Particles are simulated for 31 days and plotted at the location of their start positions.

Red areas in Figure 6 indicate regions where the biomass at the end of the simulation is less than 100%, indicating that the growth factor is on average lower than the mortality rate ($\langle \mu_{\max} f \rangle < m$ in Equation (6)). The most prominent of these negative growth areas is in the northern subtropical gyre, especially between December and May – when it is apparently too cold for the simulated *Sargassum* particles. Other growth-limited areas are near the Amazon and Mississippi rivers outflow throughout the year. Between March and May, growth is strongly limited in the equatorial region. Between August and October, particles that start in or near the Caribbean region experience a decrease in biomass.

To assess what causes the spatial variability in *Sargassum* growth in Figure 6, we create maps of the trajectory-averaged individual growth factors for the months of July 2024 and October 2024 (Figure 7). These maps show large variations.

Very clear is that the temperature growth factor (left column in Figure 7) is much lower in the eastern Caribbean in October 2024 than in July 2024. This is because of the very high temperatures in this area in late summer – temperatures that are far higher than the optimal temperature for *Sargassum* growth. This seasonality is reversed in the Northern Gulf of Mexico, where the temperature growth factor is lower in July 2024 than in October 2024.

As expected, nitrate limits growth mostly in the oligotrophic subtropical gyre (second column in Figure 7), while there is no limitation ($f_N \approx 1$) in the Canary upwelling zone, and little limitation along the equator and in the Amazon and Mississippi outflow plume. There is little difference between the spatial patterns in July 2024 and October 2024.

https://doi.org/10.5194/egusphere-2026-3097
Preprint. Discussion started: 23 June 2026

Salinity does not limit growth in most of the basin (third column in Figure 7), except for relatively small but very pronounced regions in the Amazon, Niger and Mississippi outflow and off the West-African continent and north of the Gulf Stream. Salinity is so low in these regions that it reduces f_S to near-zero, implying that there is no growth of *Sargassum* (and hence a decrease in biomass due to mortality) in these regions.

These three growth factors then multiply to the total growth factor (right column in Figure 7), which shows unlimited growth only in the eastern equatorial Atlantic Ocean and near the Canary Islands. In most of the western Tropical Atlantic Ocean, on the other hand, growth is limited to only 20-60% of its maximum potential.

4 Conclusions and discussion

In this work, we present a customizable Lagrangian simulation framework and growth model for *Sargassum*. The virtual *Sargassum* particles are advected by currents, windage and depth-integrated Stokes drift. The biological model includes growth limitation by temperature, nitrate availability and salinity. To account for mortality and sinking of *Sargassum*, a constant mortality rate is also included. The model is available as an interactive Jupyter notebook at https://doi.org/10.5281/zenodo.20441020, which supports both near-real-time simulations using the Copernicus Marine Service ocean forecasts, as well as exploring sensitivity to model parameters such as growth limitation and depth extent of the rafts.

Our results indicate that the combination of physical transport and biological growth significantly affects *Sargassum* distribution. For example, the satellite-based simulation of July 2024 shows a widespread *Sargassum* distribution near the Caribbean, yet with little to no increase in biomass. In contrast, near the African coast the distribution is spatially restricted, but the biomass increase on the virtual particles is large, in agreement with the recent finding by Beron-Vera et al. (2026). This highlights that environmental differences across the Atlantic Ocean play a significant role, and that spatial distribution is a crucial factor for the prediction of increases in *Sargassum* biomass.

As seen in Figure 2, the *Sargassum* distribution from the satellite-based initialisation after 31 days agrees reasonably with the distribution detected by satellites on 1 August 2024. The model also provides an estimate of *Sargassum* that strands on coasts vs. remaining drifting on the timescales considered in this simulation. However, there are some local differences, which may be related to the quality of the hydrodynamic data (Wang et al., 2019; Van Sebille et al., 2021; Jouanno et al., 2021), limitations in detection of *Sargassum* by remote sensing techniques such as cloud coverage and the spatial resolution of satellite imagery (Debue et al., 2025), and uncertainties in the transport itself because the physical properties (size, density and shape) of a *Sargassum* raft can differ from those of an idealized and infinitesimally small fluid tracer (Beron-Vera, 2021).

Our biological growth model shows that, on a basin-scale, the growth factor dependency on temperature is the most important for *Sargassum* growth. The high sea surface temperatures in July 2024 and October 2024 were likely a main contributor to the termination of the *Sargassum* bloom that year. Similar conclusions were drawn by Podlejski et al. (2024), who also marked temperature as the most important driver of *Sargassum* growth and found that high sea surface temperatures north of Brazil interrupt the annual growth of *Sargassum*. The timing and intensity of this warming likely contributes to the interannual

https://doi.org/10.5194/egusphere-2026-3097
Preprint. Discussion started: 23 June 2026

variation in *Sargassum* blooms (Wang et al., 2019). Although the salinity-dependent growth factor has a small effect on basin-scale (Figure 4), the maps in Figure 7 showed that salinity can have a strong growth limiting effect locally.

Upwelling areas, coastal areas and river plumes have a high nitrate growth factor, while the open ocean is less favourable for growth. Jung et al. (2025) investigated nitrogen fixation in corals and also found a strong correlation with ocean circulation, specifically with upwelling near the equator, and highlight that deep water adds more phosphorus than nitrogen, creating an environment with excess phosphorus. Excess phosphorus increases the activity of nitrogen fixating microbes, thereby increasing the amount of nitrogen in the ocean that algae can use. Jung et al. (2025) therefore argue that *Sargassum* thrives during periods of strong equatorial upwelling. This conclusion is in line with the patterns in Figure 6, where areas with high biomass growth coincide mainly with upwelling areas. Additionally, these results indicate that it is reasonable to neglect phosphorus as a limiting factor in the biological model. Similar conclusions were drawn by Lapointe et al. (2021).

While multiple studies have investigated the effect of nutrients on *Sargassum* (Lapointe et al., 2021; Magaña-Gallegos et al., 2023a; Theirlynck et al., 2025; Jung et al., 2025), there is currently less attention for the effect of salinity. However, our results indicate that the relatively fresh waters, brought into the Atlantic Ocean by the Amazon River, have a larger impact than the effect of additional nutrient supply. The occurrence of low salinity likely contributed to the termination of the *Sargassum* bloom season in 2024. These results underscore the need for further investigation into the response of *Sargassum* to salinity.

Our results demonstrate that, on timescales of several weeks, biological growth contributes substantially to the *Sargassum* distribution. As a consequence, growth should be incorporated into predictive models to improve estimates of *Sargassum* biomass reaching coastal regions or washing ashore. More accurate predictions could support more effective offshore and onshore collection projects, as well as circular use methods and valorization attempts (Oxenford et al., 2021).

Especially since *Sargassum* growth varies strongly temporarily and spatially, our framework could be used as a preliminary diagnostic tool to assess whether growth should be included in specific forecasting applications. It can provide an indication of the scales (in time and in space) at which *Sargassum* biomass will increase significantly.

Code and data availability. All code to replicate this study - and also to adapt the framework - is available on Zenodo at https://doi.org/10.5281/zenodo.20441020.

Appendix A: Additional figures

https://doi.org/10.5194/egusphere-2026-3097
Preprint. Discussion started: 23 June 2026

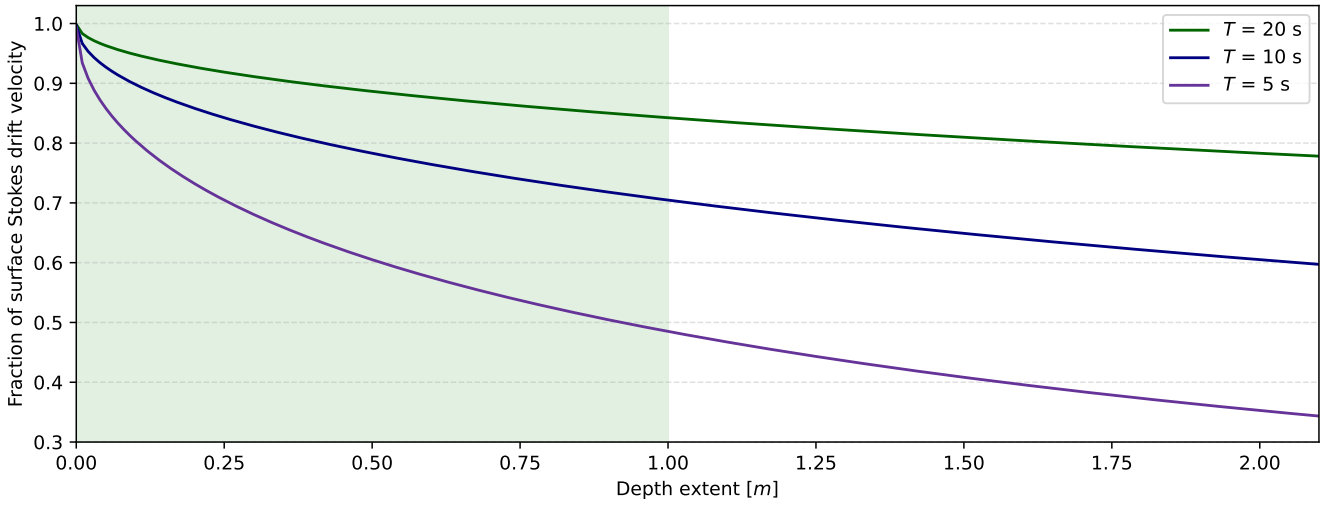

Figure A1. Analytical solutions of Stokes drift decay as a function of depth extent, following Equations (2) and (3). Results are shown for multiple wave periods (T). The upper depth extent is fixed at 0 m in all cases. Green shaded area indicates the default depth extent of *Sargassum* rafts.

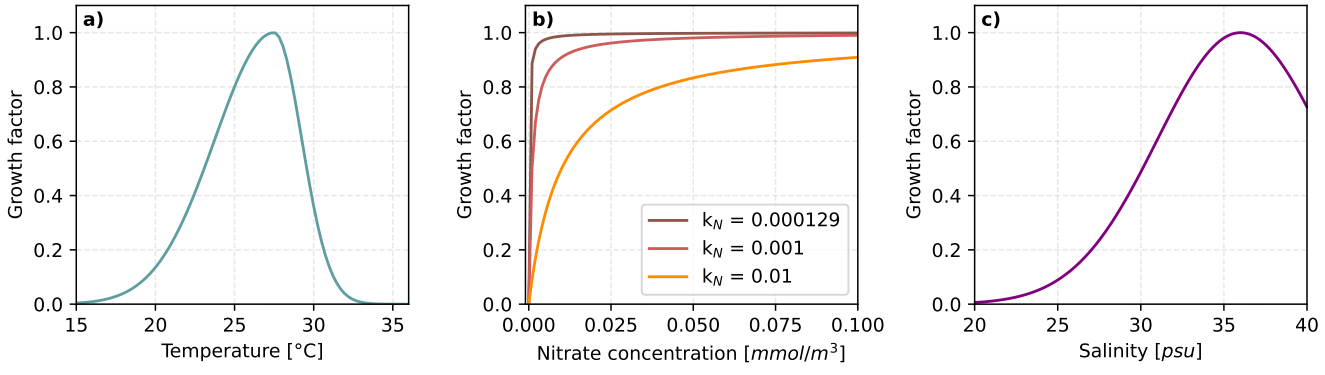

Figure A2. Growth factor dependencies on a) temperature, b) nitrate concentration as a function of k_N in the Monod Equation (9), and c) salinity.

https://doi.org/10.5194/egusphere-2026-3097
Preprint. Discussion started: 23 June 2026

Table B1. Model parameters for the Lagrangian modelling framework for *Sargassum* growth used here.

Parameter	Description	Value
Δt_{sim}	Integration timestep	10 minutes
Δt_{out}	Output timestep	2 hours
T_{sim}	Total duration of simulation	31 days
z_{upper}	Upper depth extent of *Sargassum* raft	0.0 m
z_{lower}	Lower depth extent of *Sargassum* raft	1.0 m
c	Windage coefficient	0.01
$\mu_{\max}$	Maximum growth rate	0.095 day^{-1}
m	Mortality rate	0.025 day^{-1}
T_{opt}	Optimal temperature at which growth is max	27.5 °C
$T_{\min}$	Lower temperature limit below which growth ceases	20.0 °C
$T_{\max}$	Upper temperature limit above which growth ceases	31.0 °C
S_{opt}	Optimal salinity at which growth is max	36.0 psu
k_N	Nitrate uptake half saturation	0.001 mmol/m^3

Table B2. Input variables, datasets, sources and model characteristics. Peak wave period is in the original data referred to as the wave period at spectral peak.

Variables	Model	Source	Resolution / Grid
Zonal & meridional velocity (U, V), potential temperature (T), salinity (S)	NEMO Global Ocean Physics Analysis and Forecast (GLO12 PHY_001_024)	E.U. Copernicus Marine Service Information (2024a)	1/12° Daily
Sea surface wave stokes drift zonal & meridional velocity, peak wave period	Global Ocean Waves Analysis and Forecast (WAV_001_027)	E.U. Copernicus Marine Service Information (2024b)	1/12° 3-Hourly
Mole concentration of nitrate (NO_3^-)	Global Ocean Biogeochemistry Analysis and Forecast (BGC_001_028)	E.U. Copernicus Marine Service Information (2024c)	1/4° Daily
Zonal & meridional wind velocities, 10 m above sea surface	Global Ocean Hourly Reprocessed Sea Surface Wind and Stress from Scatterometer and Model (WIND_GLO_PHY_L4_MY_012_006)	E.U. Copernicus Marine Service Information (2024d)	1/8° Hourly

https://doi.org/10.5194/egusphere-2026-3097
Preprint. Discussion started: 23 June 2026

Appendix B: Additional tables

Author contributions. EG developed the model, performed the analysis and wrote an initial thesis version of this manuscript, supervised by MB and EvS. EvS condensed and rewrote the thesis into this manuscript. LAZ, EZ and FN provided input on the biological aspects of *Sargassum* growth. All authors edited the final manuscript.

Competing interests. The authors have no competing interests

Acknowledgements. This research was supported by the Weeds of Change project (NWOCA.1) of the research program Sargassum Call 2 which is jointly financed by the Dutch Research Council (NWO), the French National Research Agency (Agence Nationale de la Recherche (ANR), and the Brazilian Fundação de Amparo a Ciência e Tecnologia do Estado de Pernambuco (FACEPE) to LAA-Z, ERZ, and EvS and financially supported the postdoctoral position of FN. EvS was also supported by the NECCTON project, which has received funding from Horizon Europe RIA under grant agreement No 101081273. The simulations were carried out on the SURF Research Cloud via project EINF-15719.

https://doi.org/10.5194/egusphere-2026-3097
Preprint. Discussion started: 23 June 2026

References

Allen, A. A. and Plourde, J. V.: Review of leeway: field experiments and implementation, Tech. rep., 1999.

Amaral-Zettler, L. A., Dragone, N. B., Schell, J., Slikas, B., Murphy, L. G., Morrall, C. E., and Zettler, E. R.: Comparative mitochondrial and chloroplast genomics of a genetically distinct form of *Sargassum* contributing to recent "Golden Tides" in the Western Atlantic, Ecology and Evolution, 7, 516–525, 2017.

Beron-Vera, F. J.: Nonlinear dynamics of inertial particles in the ocean: From drifters and floats to marine debris and *Sargassum*, Nonlinear dynamics, 103, 1–26, 2021.

Beron-Vera, F. J., Olascoaga, M. J., Miron, P., and Bonner, G.: Tracing the origin of tropical North Atlantic *Sargassum* blooms to West Africa, PNAS Nexus, 5, pgag085, https://doi.org/10.1093/pnasnexus/pgag085, 2026.

Bonner, G., Beron-Vera, F. J., and Olascoaga, M. J.: Charting the course of *Sargassum*: Incorporating nonlinear elastic interactions and life cycles in the Maxey–Riley model, PNAS nexus, 3, pgae451, 2024.

Brooks, M. T., Coles, V. J., and Coles, W. C.: Inertia influences pelagic *Sargassum* advection and distribution, Geophysical Research Letters, 46, 2610–2618, 2019.

Chávez, V., Uribe-Martínez, A., Cuevas, E., Rodríguez-Martínez, R. E., Van Tussenbroek, B. I., Francisco, V., Estévez, M., Celis, L. B., Monroy-Velázquez, L. V., Leal-Bautista, R., et al.: Massive influx of pelagic *Sargassum* spp. on the coasts of the Mexican Caribbean 2014–2020: challenges and opportunities, Water, 12, 2908, 2020.

Corbin, M. and Oxenford, H. A.: Assessing growth of pelagic *Sargassum* in the Tropical Atlantic, Aquatic Botany, 187, 103 654, 2023.

Debue, M., Guinaldo, T., Jouanno, J., Chami, M., Barbier, S., Berline, L., Chevalier, C., Daniel, P., Daniel, W., Descloitres, J., et al.: Understanding the *Sargassum* phenomenon in the Tropical Atlantic Ocean: From satellite monitoring to stranding forecast, Marine Pollution Bulletin, 216, 117 923, 2025.

Delandmeter, P. and Van Sebille, E.: The Parcels v2. 0 Lagrangian framework: new field interpolation schemes, Geoscientific Model Development, 12, 3571–3584, 2019.

Editors, N.: Tightening the *Sargassum* belt, Nature Geoscience, 18, 1181, https://doi.org/10.1038/s41561-025-01886-y, published 08 December 2025, 2025.

E.U. Copernicus Marine Service Information: Global Ocean Physics Analysis and Forecast, Marine Data Store (MDS), https://doi.org/10.48670/moi-00016, (2024a), 2024a.

E.U. Copernicus Marine Service Information: Global Ocean Waves Analysis and Forecast, Marine Data Store (MDS), https://doi.org/10.48670/moi-00017, (2024b), 2024b.

E.U. Copernicus Marine Service Information: Global Ocean Biogeochemistry Analysis and Forecast, Marine Data Store (MDS), https://doi.org/10.48670/moi-00015, (2024c), 2024c.

E.U. Copernicus Marine Service Information: Global Ocean Hourly Reprocessed Sea Surface Wind and Stress from Scatterometer and Model, Marine Data Store (MDS), https://doi.org/10.48670/moi-00185, (2024c), 2024d.

Gower, J., Young, E., and King, S.: Satellite images suggest a new *Sargassum* source region in 2011, Remote Sensing Letters, 4, 764–773, 2013.

Hanisak, M. D. and Samuel, M. A.: Growth rates in culture of several species of *Sargassum* from Florida, USA, in: Twelfth International Seaweed Symposium: Proceedings of the Twelfth International Seaweed Symposium held in Sao Paulo, Brazil, July 27–August 1, 1986, pp. 399–404, Springer, 1987.

https://doi.org/10.5194/egusphere-2026-3097
Preprint. Discussion started: 23 June 2026

Hersbach, H., Bell, B., Berrisford, P., Biavati, G., Horányi, A., Muñoz Sabater, J., Nicolas, J., Peubey, C., Radu, R., Rozum, I., et al.: ERA5 hourly data on single levels from 1940 to present, Copernicus climate change service (c3s) climate data store (cds), 10, 2023.

Hu, C., Zhang, S., Barnes, B. B., Xie, Y., Wang, M., Cannizzaro, J. P., and English, D. C.: Mapping and quantifying pelagic *Sargassum* in the Atlantic Ocean using multi-band medium-resolution satellite data and deep learning, Remote sensing of environment, 289, 113 515, 2023.

Johns, E. M., Lumpkin, R., Putman, N. F., Smith, R. H., Muller-Karger, F. E., Rueda-Roa, D. T., Hu, C., Wang, M., Brooks, M. T., Gramer, L. J., et al.: The establishment of a pelagic *Sargassum* population in the tropical Atlantic: biological consequences of a basin-scale long distance dispersal event, Progress in Oceanography, 182, 102 269, 2020.

Johnson, D. R., Franks, J. S., Oxenford, H. A., and Cox, S.-A. L.: Pelagic *Sargassum* prediction and marine connectivity in the tropical Atlantic, Gulf and Caribbean Research, 31, GCFI20–GCFI30, 2020.

Jouanno, J., Benshila, R., Berline, L., Soulié, A., Radenac, M.-H., Morvan, G., Diaz, F., Sheinbaum, J., Chevalier, C., Thibaut, T., et al.: A NEMO-based model of *Sargassum* distribution in the tropical Atlantic: description of the model and sensitivity analysis (NEMO-Sarg1. 0), Geoscientific Model Development, 14, 4069–4086, 2021.

Jouanno, J., Berthet, S., Muller-Karger, F., Aumont, O., and Sheinbaum, J.: An extreme North Atlantic Oscillation event drove the pelagic *Sargassum* tipping point, Communications Earth & Environment, 6, 95, 2025.

Jung, J., Duprey, N. N., Foreman, A. D., D'Olivo, J. P., Pellio, C., Ryu, Y., Murphy, E. L., Romshoo, B., Kersting, D. K., Cardoso, G. O., et al.: Equatorial upwelling of phosphorus drives Atlantic N2 fixation and *Sargassum* blooms, Nature Geoscience, pp. 1–7, 2025.

Lapointe, B., Brewton, R., Herren, L., Wang, M., Hu, C., McGillicuddy Jr, D., Lindell, S., Hernandez, F., and Morton, P.: Nutrient content and stoichiometry of pelagic *Sargassum* reflects increasing nitrogen availability in the Atlantic Basin, Nature Communications, 12, 3060, 2021.

Li, Q., Fox-Kemper, B., Breivik, Ø., and Webb, A.: Statistical models of global Langmuir mixing, Ocean Modelling, 113, 95–114, 2017.

Magaña-Gallegos, E., García-Sánchez, M., Graham, C., Olivos-Ortiz, A., Siuda, A. N., and van Tussenbroek, B. I.: Growth rates of pelagic *Sargassum* species in the Mexican Caribbean, Aquatic Botany, 185, 103 614, 2023a.

Magaña-Gallegos, E., Villegas-Muñoz, E., Salas-Acosta, E. R., Barba-Santos, M. G., Silva, R., and van Tussenbroek, B. I.: The effect of temperature on the growth of holopelagic *Sargassum* species, Phycology, 3, 138–146, 2023b.

Manral, D.: Life on the move: How traits and environment constrain marine species dispersal, Doctoral thesis 1 (research uu / graduation uu), Universiteit Utrecht, https://doi.org/10.33540/2801, 2025.

Marsh, R., Addo, K. A., Jayson-Quashigah, P.-N., Oxenford, H. A., Maxam, A., Anderson, R., Skliris, N., Dash, J., and Tompkins, E. L.: Seasonal predictions of holopelagic *Sargassum* across the tropical Atlantic accounting for uncertainty in drivers and processes: the SARTRAC ensemble forecast system, Frontiers in Marine Science, 8, 722 524, 2021.

Marsh, R., Oxenford, H. A., Cox, S.-A. L., Johnson, D. R., and Bellamy, J.: Forecasting seasonal *Sargassum* events across the tropical Atlantic: overview and challenges, Frontiers in Marine Science, 9, 914 501, 2022.

Ody, A., Thibaut, T., Berline, L., Changeux, T., André, J.-M., Chevalier, C., Blanfune, A., Blanchot, J., Ruitton, S., Stiger-Pouvreau, V., et al.: From In Situ to satellite observations of pelagic *Sargassum* distribution and aggregation in the Tropical North Atlantic Ocean, PLoS One, 14, e0222 584, 2019.

Oxenford, H. A., Cox, S.-A., van Tussenbroek, B. I., and Desrochers, A.: Challenges of turning the *Sargassum* crisis into gold: current constraints and implications for the Caribbean, Phycology, 1, 27–48, 2021.

https://doi.org/10.5194/egusphere-2026-3097
Preprint. Discussion started: 23 June 2026

Parr, A. E.: Quantitative observations on the pelagic *Sargassum* vegetation of the western North Atlantic, The Bulletin of the Bingham Oceanographic Collection, 6, 1939.

Podlejski, W., Berline, L., Jouanno, J., Barrier, N., and Lett, C.: Drivers of growth and decay of *Sargassum* in the Tropical Atlantic: A Lagrangian approach, Progress in Oceanography, 229, 103 364, 2024.

Putman, N. F., Lumpkin, R., Olascoaga, M. J., Trinanes, J., and Goni, G. J.: Improving transport predictions of pelagic *Sargassum*, Journal of Experimental Marine Biology and Ecology, 529, 151 398, 2020.

Stokes, G. G.: On the theory of oscillatory waves, Trans. Cam. Philos. Soc., 8, 441–455, 1847.

Theirlynck, T., Staat, L., Servania, D., Engelen, A. H., van Tussenbroek, B. I., Muyzer, G., Visser, P. M., and Amaral-Zettler, L.: Nutrient-driven growth and microbiome shifts in the brown alga *Sargassum fluitans* III, Journal of Phycology, 2025.

van den Bremer, T. S. and Breivik, Ø.: Stokes drift, Philosophical Transactions of the Royal Society A: Mathematical, Physical and Engineering Sciences, 376, 20170 104, 2018.

Van Sebille, E., Zettler, E., Wienders, N., Amaral-Zettler, L., Elipot, S., and Lumpkin, R.: Dispersion of surface drifters in the tropical Atlantic, Frontiers in Marine Science, 7, 607 426, 2021.

Van Tussenbroek, B. I., Hernández Arana, H. A., Rodríguez-Martínez, R. E., Espinoza-Avalos, J., Canizales-Flores, H. M., González-Godoy, C. E., Barba-Santos, M. G., Vega-Zepeda, A., and Collado-Vides, L.: Severe impacts of brown tides caused by *Sargassum* spp. on near-shore Caribbean seagrass communities, Marine Pollution Bulletin, 122, 272–281, https://doi.org/10.1016/j.marpolbul.2017.06.057, 2017.

van Tussenbroek, B. I., Monroy-Velázquez, L. V., Rodríguez, D., Suescún-Bolívar, L. P., Thomé, P. E., Cerqueda-García, D., García-Maldonado, J. Q., Martínez-López, I. G., López-Portillo, J. A., Barba-Santos, M. G., et al.: Monitoring drift and associated biodiversity of nearshore rafts of holopelagic *Sargassum* spp. in the Mexican Caribbean, Aquatic Botany, 195, 103 792, 2024.

Wang, M., Hu, C., Barnes, B. B., Mitchum, G., Lapointe, B., and Montoya, J. P.: The Great Atlantic *Sargassum* Belt, Science, 365, 83–87, 2019.

Winge, Ö.: The Sargasso Sea, its boundaries and vegetation, https://api.semanticscholar.org/CorpusID:127908082, 1923.